Proceedings of the 11th Brazilian Congress of Thermal Sciences and Engineering -- ENCIT 2006
Braz. Soc. of Mechanical Sciences and Engineering -- ABCM, Curitiba, Brazil,- Dec. 5-8, 2006

Paper CIT06-0360

EFFECTS OF TEMPERATURE, ATMOSPHERE AND PARTICLE SIZE ON THE KINETICS AND CONVERSION OF SULFUR DIOXIDE SORPTION BY LIMESTONE

Ivonete Ávila
Group and Thermal and Fluids Engineering, School of Engineering of São Carlos, University of São Paulo, Av. Trabalhador São-carlense 400, 13566-590, São Carlos - SP, Brazil.
iavila@sc.usp.br

Fernando Eduardo Milioli
Group and Thermal and Fluids Engineering, School of Engineering of São Carlos, University of São Paulo, Av. Trabalhador São-carlense 400, 13566-590, São Carlos - SP, Brazil.
milioli@sc.usp.br

Paula Manoel Crnkovic
Group and Thermal and Fluids Engineering, School of Engineering of São Carlos, University of São Paulo, Av. Trabalhador São-carlense 400, 13566-590, São Carlos - SP, Brazil.
paulam@sc.usp.br

Abstract. *Thermogravimetry was applied to determine the effects of temperature, atmosphere and particle size on the kinetics and conversion of sulfur dioxide sorption by limestone. Ranges of temperature and particle size were established for simulated conditions typical of fluidized bed coal combustion. The experiments were carried out in a thermogravimetric analyzer (Shimadzu-TGA-51H) under isothermal conditions for temperatures in the range from 650 to 950 °C, at local atmospheric pressure (~ 697 mmHg), in dynamic atmospheres of air and nitrogen. Two types of natural limestone (calcite and dolomite) were used in two different particles sizes: 530 and 650 μm. In all the cases, conversion grew with temperature and then started to drop as the temperature was further increased, possibly due to sintering. The conversion was always higher in nitrogen than in air atmosphere. The apparent activation energy, as indicated by the slope of the Arrhenius plot, resulted between 3.03 and 4.45 kJ/mol for the calcite, and 11.24 kJ/mol for the dolomite. The order of magnitude of the resulting activation energies suggest that the reaction is controlled by Knudsen diffusion for the calcite, and by pore molecular diffusion for the dolomite.*

Keywords. *thermogravimetry, sulfation, limestone, sulfur dioxide, chemical kinetics.*

1. Introduction

Acid rain is a critical environmental problem all over the world. This generic term covers a variety of phenomena, all of them related to atmospheric precipitation of acids. Acid rain refers to precipitations that are significantly more acid than unpolluted rain, which itself is mildly acidic due to the presence in it of dissolved atmospheric carbon dioxide, which forms carbonic acid as follows (Baird, 1998):

$$CO_2\,(g) + H_2O\,(aq) \rightarrow H_2CO_3(aq)\quad \text{[carbonic acid]} \tag{1}$$

Oxides of sulfur and nitrogen are present in significant amounts in polluted air, and both of them also react with water to produce acids. According to Kotz et al. (1994):

$$SO_2\,(g) + \tfrac{1}{2}\,O_2\,(g) + H_2O\,(l) \rightarrow H_2SO_4\,(aq)\quad \text{[sulfuric acid]} \tag{2}$$

$$2\,NO_2\,(g) + H_2O\,(l) \rightarrow HNO_3\,(aq)\ \text{[nitric acid]} + HNO_2\,(aq)\ \text{[nitrous acid]} \tag{3}$$

Reactions (2) and (3) are responsible for acid rain in industrialized regions. Sulfur dioxide (SO2), a pollutant that is a major contributor to acid rain, is produced when sulfur or sulfur-containing compounds are burned in air (Kotz et al., 1994).

Sulfur compounds are generally responsible for major damages to materials. Sulfur oxides generally accelerate corrosion by first forming sulfuric acid either in the atmosphere or on the surfaces of materials. Depending on the kind of material exposed as well as the duration of exposure, corrosion rates in urban sites have been observed to be from 1.5 to 5 times the rates observed in rural environments (Wark et al., 1998). Analysis of numerous epidemiological studies clearly indicate an association between air pollution, as measured by the concentration of SO_2 plus particulate matter and moisture, and health effects of varying severities. Various animal species, including humans, respond to sulfur dioxide by developing bronchoconstriction diseases (Wark et al., 1998).

Mineral coals and heavy oils from petrol are widely used for energy generation. Those fossil fuels are burned in thermoelectric power stations and are the main source of SO_2 emission into earth's atmosphere (Li and Sadakata, 1999). The development of efficient, economic and environment-friendly technologies is essential for the utilization of high-sulfur fuels. Fluidized bed combustion is one of such a technologies. It allows to remove sulfur during combustion by injecting limestone in the combustion chamber. Limestone sorbs SO_2 before it can be emitted to atmosphere (Van Houte and Delmon, 1979; Baird, 1998).

High temperature sorption of SO_2 by limestone involves reactions of calcination followed by sulfation. When submitted to high temperatures, limestone decomposes into a solid mostly formed of CaO, and the gas CO_2. The calcination reaction is given by:

$$CaCO_3\ (s) \rightarrow CaO\ (s) + CO_2\ (g) \qquad \Delta H = +\ 182.1\ kJ\ mol^{-1} \tag{4}$$

The produced calcine is very porous and has the same size of the original limestone, so that its high porosity is due to the difference between the molar volumes of $CaCO_3$ (~ 36.9 $cm^3\ mol^{-1}$) and CaO (~16.9 $cm^3\ mol^{-1}$) (Hartman and Coughlin, 1976; Simons et al., 1987; Dam-Johansen and Ostergaard, 1991). Depending on temperature and SO_2 partial pressure, different chemical species may be produced from the reaction between CaO and SO_2. The most commonly assumed routes for sulfation are:

$$\begin{aligned} &CaO\ (s) + SO_2\ (g) \rightarrow CaSO_3\ (s) \\ &CaSO_3\ (s) + \tfrac{1}{2}\, O_2\ (g) \rightarrow CaSO_4\ (s) \end{aligned} \tag{5}$$

$$\begin{aligned} &SO_2\ (g) + \tfrac{1}{2}\, O_2\ (g) \rightarrow SO_3\ (g) \\ &CaO\ (s) + SO_3\ (g) \rightarrow CaSO_4\ (s) \end{aligned} \tag{6}$$

$$\begin{aligned} &4CaO\ (s) + 4SO_2\ (g) \rightarrow 4CaSO_3\ (s) \\ &4CaSO_3\ (s) \rightarrow 3CaSO_4\ (s) + CaS\ (s) \end{aligned} \tag{7}$$

According to Dennis and Hayhurst (1990), routes (5) and (6) were proposed by Moss (1975), while route (7) was proposed by Low et al. (1971). As remarked by Anthony and Granatstein (2001), Moss suggested that the reactions of route (5) predominate at low temperatures where $CaSO_3$ is stable, while the reactions of route (6) predominate at high temperatures (>850 °C) where $CaSO_3$ becomes unstable.

During sulfation the pores of the CaO particle are filled with products ($CaSO_4$, $CaSO_3$, CaS), and become progressively plugged. Even compared to the natural limestone, the physical structure of the sulfated regions in a particle become more compact owing to the difference between the molar volumes of $CaSO_4$ (~ 46 $cm^3\ mol^{-1}$) and $CaCO_3$ (~36.9 $cm^3\ mol^{-1}$) (Dam-Johansen and Ostergaard, 1991).

Limestone sulfation is affected by porosity, size and size distribution of pores, intra-particle superficial area (Borgwardt and Bruce, 1986; Adánez et al., 1993; Li and Sadakata, 1999), geological age, size and density of the particles (Yrjas et al., 1995). Another factor to consider is the presence of chemical elements that may act as catalysts or poisons (Dam-Johansen and Ostegaard, 1991). The first works showing the influence of internal pore structure on CaO reaction to SO_2 were performed in the early 70's. With that, intrinsic physical features started to be considered alongside with the usual external superficial effects (Borgwardt and Bruce, 1986). In one of the first works, Pigford and Sliger (1973) found that in 96 μm limestone particles there was significant resistance to intra-particle gas diffusion at 980 °C. The authors concluded that SO_2 diffusion through the $CaSO_4$ product layers controlled sulfation rate. Borgwardt and Harvey (1972) evaluated the effect of porosity on sulfation. They defined an effectiveness factor as the ratio between the observed reaction rate, and its theoretical value if the whole particle volume was available for reaction. A strong dependence was observed between effectiveness and pore structure (volume, area and shape of pores). The authors concluded that the effectiveness was dependent on external layers pore plugging by $CaSO_4$, which imposes loss of internal superficial area, and make the internal layers of CaO inaccessible.

The search for reaction controlling steps and kinetic parameters for SO_2 sorption by limestones has been undertaken by various researchers. Commonly reported apparent activation energies vary in a wide range, from unities to hundreds of kJ mol^{-1}. Several works report apparent activation energies obtained through thermogravimetry in various operational conditions, e.g.: 133 kJ mol^{-1} between 650 and 800 °C (Iisa and Hupa, 1992); 146 kJ mol^{-1} for conversion above 50 % (Hajaligol et al., 1988); 64 kJ mol^{-1} for direct sulfation, and 205 kJ mol^{-1} for sulfation preceded of calcination (Snow et al., 1988); 95±14, 77±20 and 70±21 kJ mol^{-1} for direct sulfation in atmospheres containing, respectively, 30, 50 and 80 % CO_2, between 500 and 850 °C (Tullin et al., 1993). Crnkovic (2003) applied thermogravimetry to evaluate the sulfation of a calcitic and a dolomitic limestone. Samples of particulate with sizes between 390 and 779 μm were submitted to process temperatures between 600 and 900 °C. In the sulfation of a dolomitc previously calcined 650 μm limestone, in SO_2 atmosphere, the apparent activation energy at the maximum reaction rate condition resulted 5.3 kJ mol^{-1} (between 600 and 700 °C), and 11.6 kJ mol^{-1} (between 700 and 850 °C).

The activation energy in heterogeneous fluid-solid reactions is commonly addressed as apparent since it is highly affected by intra-particle mass transport. Pore plugging, sintering and particle size become crucial (James and Hughes, 1976; Iisa and Hupa, 1992; Crnkovic, 2003; Crnkovic et al., 2006). Fuertes et al. (1994) notes a literature agreement (Bhatia and Permutter, 1981, Pigford and Sliger, 1973, Gopalakrishanan and Seehra, 1990) on that the high reported activation energies for calcine sulfation (between 121 and 167 kJ mol^{-1}) are not satisfactorily explained by diffusion control. The authors observe that, under molecular diffusion control, the activation energies result around 12 kJ mol^{-1}, while under Knudsen diffusion control, they result around 4 kJ mol^{-1}.

Dennis and Hayhurst (1990) determined conversions and reaction rate coefficients for the sorption of SO_2 by limestone in a fluidized bed reactor electrically heated, in atmospheres containing variable concentrations of O_2 and N_2. They found that by decreasing O_2 concentration, the conversion increases, while the drop of reaction rate coefficient becomes slower in time. The authors concluded, however, that the presence of a small amount of O_2 accelerates the sulfation without causing significant decrease on conversion. Lindo (2003) studied the effect of the concentration of SO_2 on the direct sulfation of limestones in a bench fluidized bed reactor. The author found a quicker and more effective sulfation when SO_2 was present in higher concentrations. Supposedly, at higher concentrations of SO_2 pore plugging is intensified at the outer layers of the particles, forming thinner sulfated shells. As CO_2 flows out from the particles, it becomes easier for the gas to break through thinner shells, causing cracks and providing a path for SO_2 penetration. Costa (2000) studied the effect of temperature on conversion and reaction rate coefficient for the sorption of SO_2 by limestone in a bench fluidized bed. The author used a calcitic limestone which is also applied in the present study (the limestone named CI). The reaction rate coefficient for 650 µm limestone particles resulted maximum at 881 °C.

The purpose of this work is to use thermogravimetry to analyze the influence of temperature, atmosphere and particle size on conversion and kinetics of SO_2 sorption by previously calcined limestone. The ranges of temperature and particle size applied are typical of fluidized bed coal combustion.

2. Materials and Experiments

Two types of Brazilian natural limestones were used: a calcitic limestone named CI, and a dolomitic limestone named DP. Table (1) shows the elementary chemical compositions of the limestones CI and DP which were determined by atomic emission spectrometry (ICP-AES).

Table 1. Elementary chemical composition (% mass/mass) of the limestones.

Limestones	Chemical Composition						
	Ca	Mg	Fe	Al	Sr	K	Mn
CI	35.34	0.35	2.45	0.25	0.14	0.09	0.52
DP	17.07	11.73	0.32	0.42	0.08	0.13	0.09

The thermogravimetric experiments were performed in a Shimadzu TGA-51H analyzer. Limestone Samples weighing 10.0±0.5 mg were used throughout the experiments. This allowed to minimize inter-particle mass transfer resistances by spreading the particles in a monolayer on the bottom of the pan (alumina, 6∅ × 2.5 mm). The limestone CI was used in two different mean sizes: 545 µm and 650 µm; the limestone DP was 650 µm mean size. Previously to sulfation, the sample was calcined inside the analyzer in air or nitrogen atmospheres, at a volumetric rate of 80 mL min^{-1}, applying a heating rate of 30 °C min^{-1}, until a desired temperature was reached and the decomposition was complete. This condition was kept for 20 min. Then, 20 mL min^{-1} of SO_2 was added so that it's a volumetric fraction was 20%, and the isothermal sulfation developed. Five different sulfation temperatures were performed (750, 800, 850 and 900 °C), and three replicates were carried out on each temperature.

2. Methodology

2.1. Conversion

In this work, the conversion (*X*) of a reactant *"i"* indicates the ratio between the number of moles of the species which reacts and the number of moles of the species fed in the process. Then, the conversion is given by:

$$X(\%) = \frac{\text{moles of "i" that react}}{\text{moles of "i" fed in the process}} \times 100 \tag{8}$$

In the present thermogravimetric sulfation experiments the conversion of Ca plus Mg is given by:

$$X = \frac{\left(n_{Ca} + n_{Mg}\right)_{\text{reacted}}}{\left(n_{Ca} + n_{Mg}\right)_{\text{in the sample}}} \times 100 = \frac{\left(n_{SO_2}\right)_{\text{sorbed}}}{\left(n_{Ca} + n_{Mg}\right)_{\text{in the sample}}} \times 100 \ , \tag{9}$$

where n stands for the number of moles of a concerning species. It should be noted that, irrespective of the considered reaction mechanism, the number of moles of SO_2 that is sorbed equals the number of moles of Ca plus Mg that is reacted.

The injection of SO_2 in the thermogravimetric analyzer promotes sulfation, causing mass increase. Thus, the total mass variation due to the sulfation of the already calcined sample (ΔM_S) is given by:

$$\Delta M_S = M_{SO_2} + M_{O_2} = n_{SO_2} W_{SO_2} + n_{O_2} W_{O_2} \tag{10}$$

Given the global reaction:

$$\text{CaO (or MgO)} + SO_2 + \tfrac{1}{2} O_2 \rightarrow CaSO_4 \text{ (or } MgSO_4\text{)}, \tag{11}$$

it comes that:

$$\frac{n_{SO_2}}{n_{O_2}} = \frac{1}{\frac{1}{2}} \therefore n_{O_2} = \tfrac{1}{2} n_{SO_2} \tag{12}$$

Substituting Eq. (12) into Eq. (10):

$$n_{SO_2} = \frac{\Delta M_S}{\left(W_{SO_2} + \frac{1}{2} W_{O_2}\right)}, \tag{13}$$

where W stands for the molecular mass of the concerning species. The total mass variation due to sulfation, ΔM_S, is also given by:

$$\Delta M_S = M_F - M_C \ , \tag{14}$$

where M_F is the final sample mass after sulfation, and M_C is the mass of the sample after calcination.

The number of moles of Ca plus Mg available in the sample is given by:

$$n_{Ca} + n_{Mg} = M_A \left(\frac{Y_{Ca}}{W_{Ca}} + \frac{Y_{Mg}}{W_{Mg}} \right), \tag{15}$$

where M_A is the initial sample mass of the natural limestone, Y stands for mass fractions, and W account for atomic masses.

Introducing Eq. (13) and Eq. (15) in Eq. (9), it comes that:

$$X = \frac{\dfrac{M_F - M_C}{W_{SO_2} + \frac{1}{2} W_{O_2}}}{M_A \left(\dfrac{Y_{Ca}}{W_{Ca}} + \dfrac{Y_{Mg}}{W_{Mg}} \right)} \times 100 \tag{16}$$

This equation stands for conversion in air atmosphere. To account for nitrogen atmosphere, the term $\frac{1}{2} W_{O_2}$ must be dropped from Eq. (16).

2. 2. Kinetics

In this work Arrhenius kinetics is applied. Therefore, the reaction rate coefficient is given by:

$$k = A \, exp\left(-\frac{E_a}{RT} \right), \tag{17}$$

where A is the pre-exponential or frequency factor, E_a is the apparent activation energy, R is the ideal gas constant, and T is the temperature. The reaction rate may be given by:

$$-\frac{dm}{dt} \propto m^a \, C_{SO_2}^b \, C_{O_2}^c \tag{18}$$

where m is the mass of Ca plus Mg available for sulfation, dm/dt is the reaction rate of Ca plus Mg, C is the concentration of gases (SO_2 and O_2) in the atmosphere, and (a, b, c) represent the order of the global reaction in relation to m and C. Following literature of gas-solid reaction, first order reaction is considered regarding the mass of the sample (Levenspiel, 1972). Also, differential conditions are considered (Borgwardt, 1985), so that the reaction rate is assumed to be independent of the concentration of reactant gases. Therefore, the reaction is assumed of order zero regarding the concentrations of gases. Under those assumptions, the reaction rate becomes:

$$-\frac{dm}{dt} \propto m \tag{19}$$

Introducing a reaction rate coefficient (k) in Eq. (19), it comes:

$$-\frac{dm}{dt} = k\,m \tag{20}$$

Inserting Eq. (17) into Eq. (20), and applying the *ln* operator, it follows that:

$$ln\left[-\frac{1}{m}\frac{dm}{dt}\right] = ln\,A - \frac{E_a}{R}\frac{1}{T} \tag{21}$$

Through a mass balance, and assuming that Ca and Mg are consumed at the same rate, the available mass of Ca plus Mg available for reaction can be found as:

$$m = M_A\left(Y_{Ca} + Y_{Mg}\right) - \left(M - M_C\right)\left[\frac{\left(W_{Ca}Y_{Ca} + W_{Mg}Y_{Mg}\right)}{\left(W_{SO_2} + \tfrac{1}{2}W_{O_2}\right)\left(Y_{Ca} + Y_{Mg}\right)}\right], \tag{22}$$

where M is the mass of the sample variable during sulfation. From Eq. (22) it comes that:

$$\frac{dm}{dt} = -\left[\frac{\left(W_{Ca}Y_{Ca} + W_{Mg}Y_{Mg}\right)}{\left(W_{SO_2} + \tfrac{1}{2}W_{O_2}\right)\left(Y_{Ca} + Y_{Mg}\right)}\right]\frac{dM}{dt} \tag{23}$$

Equation (23) stands for air atmosphere. To account for nitrogen atmosphere the term $\tfrac{1}{2}W_{O_2}$ must be dropped from the equation.

From the empirical data and applying Eq. (8) an Arrhenius plot is defined. Then, by linear regression both the pre-exponential factor and the activation energy are determined.

The required values of M_A, M_C, M and dM/dt are taken from the thermogravimetric experiments. The mass fractions of Ca and Mg in the sorbents, and the molecular weights of the concerning species are given in Tab. (2).

Table 2. Mass fractions of Ca and Mg in the limestone, and atomic and molecular weights.

Limestones	Y_{Ca}	Y_{Mg}	W_{Ca}	W_{Mg}	W_{SO_2}	W_{O_2}
Calcite (CI)	0,3534	0,0035	40,078	24,305	64,064	31,998
Dolomite (DP)	0,1707	0,1173				

3. Results

Figure (1) shows the result of the sulfation experiments performed for one of the considered temperatures (900 °C) in air atmosphere, for limestone DP of 650 μm. The sets of curves for all the other experiments resulted similar. The TG curve in Fig. (1) shows both the calcination and the sulfation events. It shows also DTG and ΔT profiles. For the purposes of this study, the data were analyzed from complete calcination to complete sulfation.

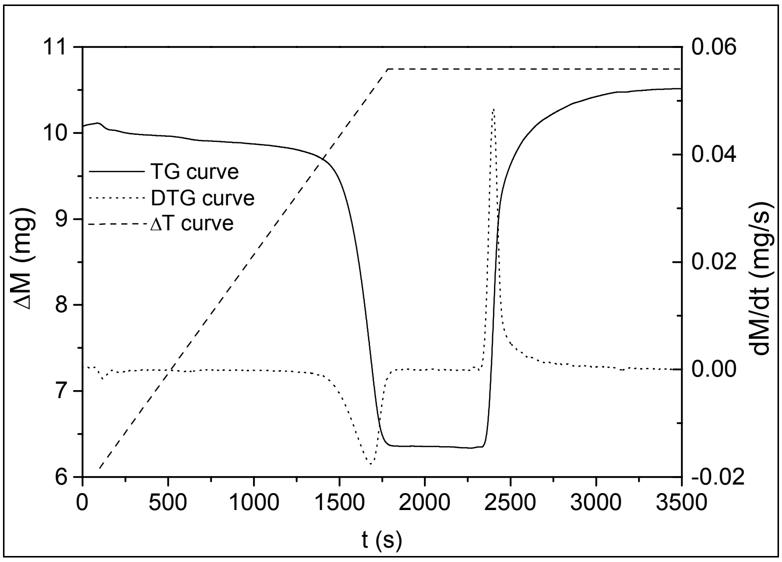

Figure 1. TG and DTG profiles of sulfation at 900 °C, of the 650 μm limestone DP, in air atmosphere.

3.1. Conversion

Conversion was calculated over a time interval set from the beginning to the end of the sulfation. The initial time was set at 100 seconds before the maximum peak of the DTG curve, when the sulfation was about to begin. The final time was set at 400 seconds after the initial time when, for practicable purposes, the sulfation was assumed to be finished. In fact, above the final time sulfation proceeded, but at a very slow rate.

Fugures (2) and (3) show TG profiles of sulfation at various temperatures, for the 545 μm limestone CI, respectively in air and nitrogen atmospheres. The curves in Fig. (2) and Fig. (3) account for averages of four replicates. Figures (4) and (5) also show TG profiles of sulfation at various temperatures, but both in air atmosphere, and respectively for the 650 μm limestones CI and DP. The curves in Fig. (4) and Fig. (5) account for averages of three replicates.

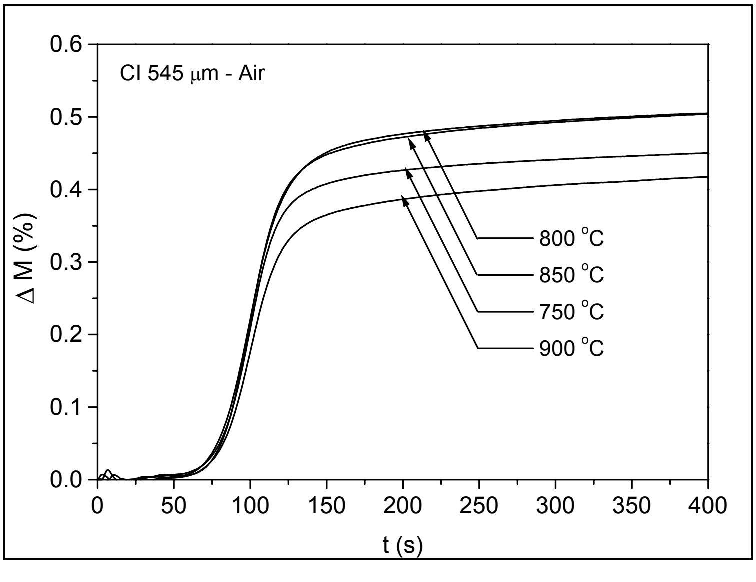

Figure 2. TG profiles of sulfation at various temperatures, for the 545 μm limestone CI, in air atmosphere. Each curve accounts for the average of four replicates.

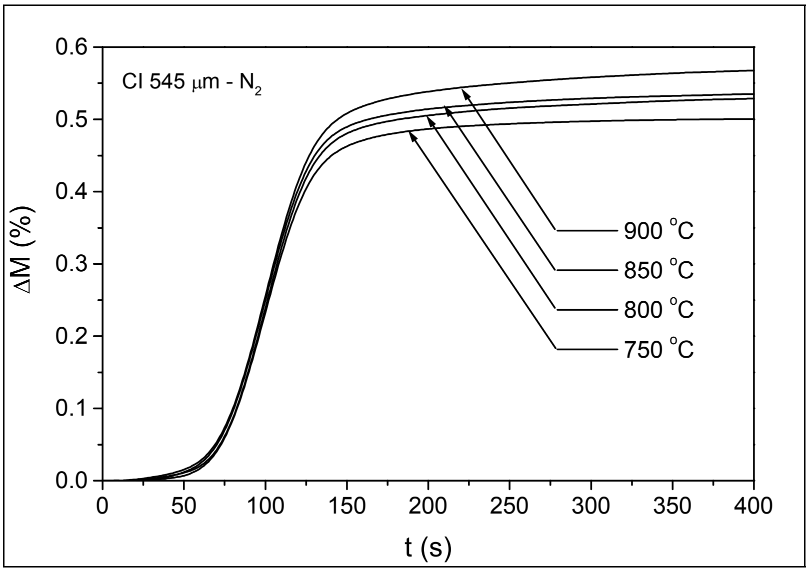

Figure 3. TG profiles of sulfation at various temperatures, for the 545 μm limestone CI, in nitrogen atmosphere. Each curve accounts for the average of four replicates.

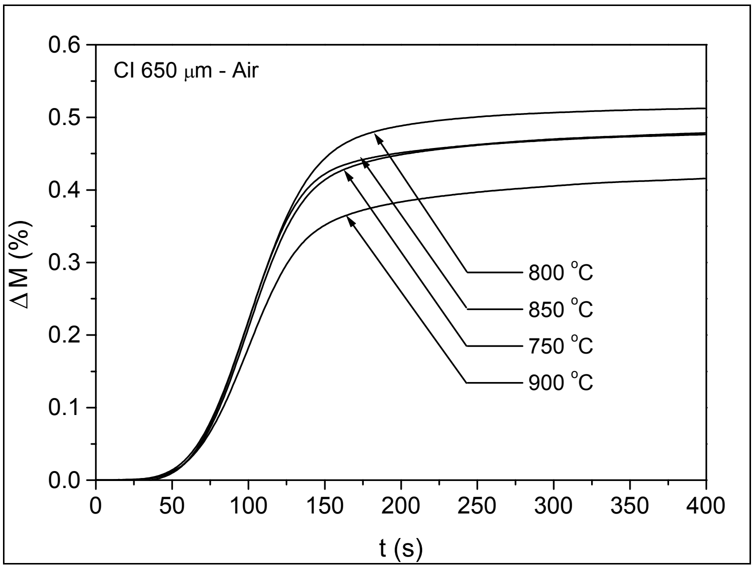

Figure 4. TG profiles of sulfation at various temperatures, for the 650 μm limestone CI, in air atmosphere. Each curve accounts for the average of three replicates.

All the curves in Fig. (2) to Fig. (5) show the same time behavior, irrespective of temperature, atmosphere, particulate size and type of limestone. Otherwise, the final gain of mass was quite different for different temperatures. Table (3) shows a decreasing rank of mass gain regarding temperature. Table (4) shows the conversion calculated for all the considered cases. Figure (6) brings plots of the conversion as a function of temperature. From polynomial fits on the curves of Fig (6) maximum conversion temperatures were found which are presented in Tab. (5).

In air atmosphere, conversion at 900 °C resulted lower than that at 800 °C for all the limestones. For the 545 μm limestone CI it resulted even lower than that at 750 °C. This fact is possibly due to sintering, which causes loss of internal superficial area and consequent conversion drop. As this behavior was not observed in nitrogen atmosphere up to 900 °C, an additional experiment was made in this atmosphere at the higher temperature of 950 °C. The conversion for this case resulted lower than that at 800 °C, showing that in nitrogen atmosphere sintering takes place at a slightly higher temperature. In both air and nitrogen atmospheres the conversion grows up with temperature and then stats to drop as temperature further increases. The temperature at which conversion starts to drop defines the maximum conversion, and represents the optimum sorption temperature.

In all temperatures, conversion resulted always higher in nitrogen than in air atmosphere. Different reaction mechanisms may account for that. In air atmosphere routes (5), (6) and (7) may take place, while in the absence of O_2 only route (7) is relevant.

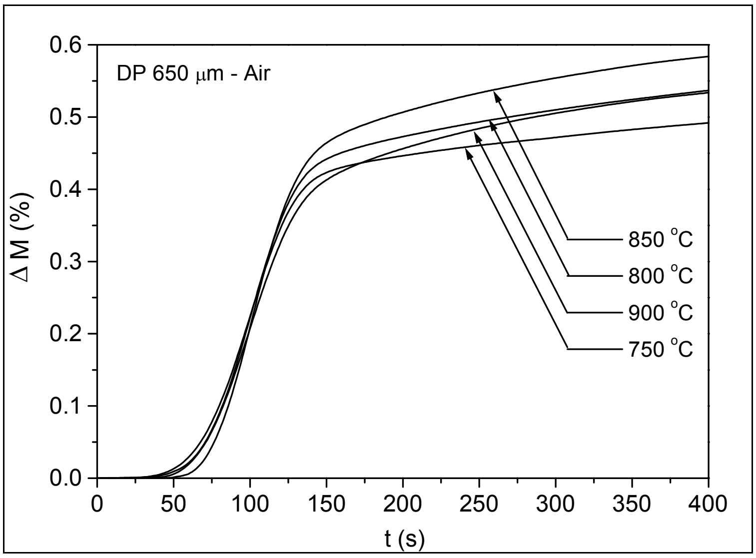

Figure 5. TG profiles of sulfation at various temperatures, for the 650 μm limestone DP, in air atmosphere. Each curve accounts for the average of three replicates.

Table 3. Decreasing rank of mass gain from Fig. (2) to Fig. (5).

Type of Limestone	Decreasing rank of mass gain
CI 545 μm – Air atmosphere	800 ≈ 850 > 750 > 900 °C
CI 545 μm – Nitrogen atmosphere	900 > 850 > 800 > 750 °C
CI 650 μm – Air atmosphere	800 > 850 ≈ 750 > 900 °C
DP 650 μm – Air atmosphere	850 > 800 > 900 > 750 °C

Table 4. Conversion for all the cases in Fig. (2) to Fig. (5), plus an additional case for the 545 μm limestone in air at 950 °C.

T (°C)	Conversion (%) $\left[\frac{\text{mols of (Ca + Mg) reacted}}{\text{mols of (Ca + Mg) in the sample}}\times 100\right]$			
	DP 650 μm - Air	CI 650 μm - Air	CI 545 μm – Air	CI 545 μm – N_2
750	47.2	38.0	38.7	51.5
800	50.1	40.5	41.4	55.0
850	50.8	37.9	41.2	56.6
900	47.6	33.4	34.6	58.4
950	-	-	-	54.6

Comparing the results of limestone CI for the different particulate sizes in Tab. (4) and Tab. (5) and Fig. (6), it is seen that a higher conversion is found for the smaller particulate, as expected. For the smaller particulate a higher external superficial area is available for reaction, meaning that a larger volume of the particles is sulfated since the thickness of the sulfated layer is independent of particle size.

Regarding the type of sorbent, conversion resulted always higher for the limestone DP in comparison to the limestone CI of the same size, in all the temperatures. Besides chemical composition, the superior performance of limestone DP may be due to a more favorable structure of pores developed during calcination and/or sulfation. Those are aspects to be further investigated.

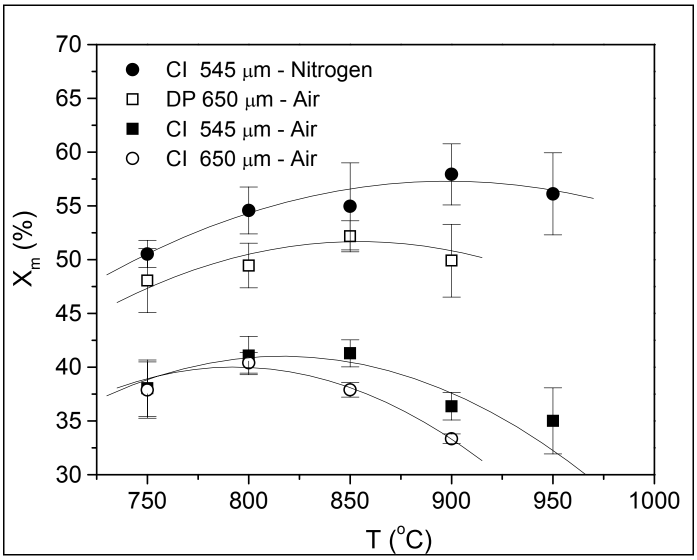

Figure 6. Conversion as a function of temperature for the various cases. The bars indicate the standard deviation around the average from the experiments. The full lines stand for polynomial fits.

Table 5. Maximum conversion temperatures from the polynomial fits of Fig (6).

Type of Limestone	Optimum Conversion Temperature
CI 545 μm – Nitrogen atmosphere	894 °C
DP 650 μm – Air atmosphere	859 °C
CI 545 μm – Air atmosphere	818 °C
CI 650 μm – Air Atmosphere	792 °C

3. 2. Kinetics

Figure (7) shows the Arrhenius plots for the various cases considered. In all the cases in air atmosphere, the reaction rate increases with temperature for temperatures up to 850 °C. Above 850 °C the reaction rate considerably drops, indicating either a change on reaction mechanism or sintering.

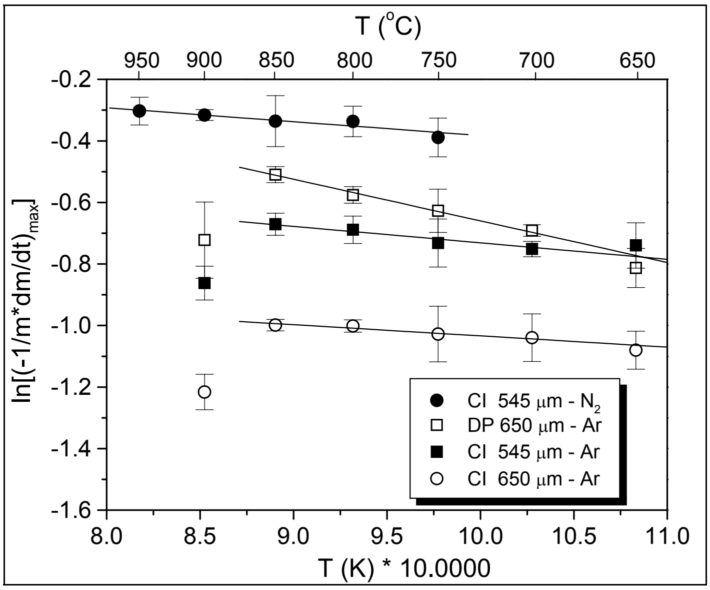

Figure 7. Arrhenius plots for the various cases considered. The bars indicate the standard deviation around the average from the experiments.

For the cases in air atmosphere, kinetic parameters were found for temperatures up to 850 ^{o}C. Additional experiments were performed at the temperatures of 650 and 700 ^{o}C to make the results more representative. Therefore, for the cases in air atmosphere the kinetic parameters stand for temperatures between 650 and 850 ^{o}C. For the case in nitrogen atmosphere the kinetic parameters stand for temperatures between 750 and 950 ^{o}C. For the various cases, the apparent activation energies and frequency factors result:

Limestone DP 650 μm in Air:

$$k_{\max}(T) = 1.997\exp\left(-\frac{11.24}{\mathrm{RT}}\right) \tag{24}$$

Limestone CI 650 μm in Air:

$$k_{\max}(T) = 0.5512\exp\left(-\frac{3.03}{\mathrm{RT}}\right) \tag{25}$$

Limestone CI 545 μm in Air:

$$k_{\max}(T) = 0.822\exp\left(-\frac{4.45}{\mathrm{RT}}\right) \tag{26}$$

Limestone CI 545 μm in N_2:

$$k_{\max}(T) = 1.071\exp\left(-\frac{3.75}{\mathrm{RT}}\right) \tag{27}$$

In air atmosphere, limestone DP presented a frequency factor about 3.6 times higher than that of the limestone CI of the same size. So, limestone DP was more than 3 times more effective than limestone CI. Otherwise, the apparent activation energy for limestone DP resulted about 3.7 times higher than that of limestone CI. Then, limestone DP required more than 3 times more energy for the reaction to be deployed.

Changing the particulate size from 650 to 545 μm, for limestone CI in air atmosphere, caused both the frequency factor and the apparent activation energy to increase. So, the smaller size was more effective, while requiring more energy for the reaction to be deployed.

Changing the atmosphere from air to nitrogen, for the 545 μm limestone CI, caused the frequency factor to increase and the activation energy to decrease. So, in nitrogen atmosphere sulfation was more effective and required less energy to be deployed.

For the limestone CI the activation energies resulted between 3.03 and 4.45 kJ mol^{-1}. This range is compatible with literature results for reaction controlled by Knudsen diffusion (around 4 kJ mol^{-1} according to Fuertes et al., 1994). For the limestone DP the activation energy resulted 11.24 kJ mol^{-1}. This value is compatible with literature results for reaction controlled by pore molecular diffusion (around 12 kJ mol^{-1} according to Fuertes et al., 1994).

4. Conclusions

The thermogravimetric sulfation experiments showed that conversion resulted always higher in nitrogen than in air atmosphere, irrespective of temperature. Different reaction mechanisms were supposed to account for that. Smaller particles improved conversion by providing larger superficial areas. The calcitic limestone CI provided better conversion than the dolomitic limestone DP. This may be attributed to different chemical compositions, besides different pore structures developed during calcination and/or sulfation. For both the limestones, in all the tested conditions, conversion started to drop above a given temperature, possibly due to sintering.

The kinetic analysis showed that, in comparison to limestone CI, limestone DP presented higher frequency factor and higher apparent activation energy. A smaller particulate size for the limestone CI caused both frequency factor and apparent activation energy to increase. Also for limestone CI, changing the atmosphere from air to nitrogen caused the frequency factor to increase and the apparent activation energy to decrease. Considering the order of magnitude of the apparent activation energies, it was concluded that the sulfation of limestone CI was controlled by Knudesn diffusion, while the sulfation of the limestone DP was controlled by pore molecular diffusion.

5. Acknowledgement

This work was supported by The State of São Paulo Research Foundation (FAPESP) and The National Council for Scientific and Technological Development (CNPq).

6. Reference list

Adánez, J., Garciá-Labiano, F. and Gayán, P., 1993, "Sulfur retention in AFBC. Modelling and sorbent characterization methods", Fuel Processing Technology, No. 36, pp. 73-79.

Anthony, E. J. and Granatstein, D. L., 2001, "Sulfation phenomena in fluidized bed combustion systems", Progress in Energy and Combustion Science, No. 27, pp. 215-236.

Borgwardt, R. H., 1985, "Calcinarion kinetics and surface area of dispersed limestone particles", AIChE, Vol. 31, No.1, pp. 103-111.

Borgwardt, R. H. and Bruce, K. R., 1986, "Effect of specific surface area on the reactivity of CaO with SO_2", AIChE J., Vol. 32, pp. 239-246.

Borgwardt, R. H. and Harvey, R. D., 1972, "Properties of carbonate rocks to SO_2 reactivity", Env. Sc. Tech., No. 6, pp. 350-360.

Braun, R. L. and Burnham, A., 1987, K. Energy & Fuels, No. 1, pp. 153-161. (apud Burnham and Braun, 1999)

Costa, M. C. D., 2000, "Efeito da temperatura sobre a conversão e o coeficiente de taxa de reação na absorção de SO_2 por calcário em reator de leito fluidizado", Dissertação de Mestrado, EESC-USP, 174 p.

Crnkovic, P. C. G. M., 2003, "Análise termogravimétrica para a determinação de fatores que afetam a eficiência de sorção de SO_2 por calcários na combustão de carvões", Tese de Doutorado, IQSC-USP, 127 p.

Crnkovic, P. M., Milioli, F. E. and Pagliuso, J. D., 2006, "Kinetics study of the SO_2 sorption by Brazilian dolomite using thermogravimetry", Thermochimica Acta (accepted for publication).

Dam-Johansen, K. and Ostergaard, K., 1991, "High-temperature reaction between sulphur dioxide and limestone – I. Comparison of limestones in two laboratory reactors and a pilot plant", Chemical Engineering Science, No. 46, No. 3, pp. 827-837.

Dam-Johansen, K. and Ostergaard, K., 1991, "High-temperature reaction between sulphur dioxide and limestone – II. An improved experimental basis for a mathematical model", Chemical Engineering Science, Vol. 46, No.3, pp. 839-845.

Dam-Johansen, K. and Ostergaard, K., 1991, "High-temperature reaction between sulphur dioxide and limestone – III. A grain-micrograin model and its verification", Chemical Engineering Science, Vol. 46, No. 3, pp. 847-853.

Dam-Johansen, K. and Ostergaard, K., 1991, "High-temperature reaction between sulphur dioxide and limestone – IV. A discussion of chemical reaction mechanisms and kinetics", Chemical Engineering Science, Vol. 46, No. 3, pp. 855-859.

Dennis, S. and Hayhurst, A.N., 1990, "Mechanism of the sulphation of calcined limestone particles in combustion gases", Chemical Engineering Science, No. 45, pp. 1175-1187.

Fuertes, A. B., Velasco, G., Fuente, E. and Alvarez, T., 1994, "Study of the direct sulfation of limestone particles at high CO_2 partial pressures", Fuel Processing Technology, Vol. 38, pp. 181-192.

Hajaligol, M. R., Longwell, J. P. and Sarofim, A. F., 1988, "Analysis and modelling of the direct sulfation of $CaCO_3$", Ind. Eng. Chem. Res., No. 27, pp. 2203-2210.

Hartman, M. and Coughlin, R. W., 1976, "Reaction of sulfur dioxide with limestone and the grain model", AIChE J., Vol. 22, No. 3, pp. 490-498.

Iisa, K. and Hupa, M., 1992, "Rate-limiting processes for the desulphurisation reaction at elevated pressures", J. Inst. Energy, No. 65, pp. 201-205.

James and Hughes, 1976, paper presented at 2nd. Int. Conf. on Conf. of Gaseous Sulphur and Nitrogen Compound Emission, Salford (1979), apud Van Houte and Delmon (1979).

Levenspiel, O., 1972, "Chemical reaction engineering", John Wiley & Sons, NY.

Li, Y. and Sadakata, M., 1999, "Study of gypsum formation of appropriate dry desulfurization process of flue gas", Fuel, No. 78, pp. 1089-1095.

Lindo, J. E. S., 2003, "Efeito da concentração de SO_2 nas reações de calcinação e sulfatação de calcários em reator de leito fluidizado", Dissertação de Mestrado, EESC-USP, 116 p.

Moss, G., 1975, "The mechanism of sulphur absorption in fluidized beds of lime", Institute of Fuel Symposium Series, No. 1: Fluidised Combustion, D2.

Pigford, R. and Sliger, G., 1973, Rate of diffusion-controlled reaction between a gas and a porous solid sphere- reaction of SO2 with CaCO3", Ind. Eng. Chem. Process Des. Develop, Vo. 12-1, pp. 85-91.

Silva, G. F. da, 2001, "Efeito do tamanho de partículas na conversão e no coeficiente global de taxa de reação na absorção de SO_2 por calcário em reator de leito fluidizado", Dissertação de Mestrado, EESC-USP, 106 p.

Simons, G. A., Garman, A. R. and Boni, A. A., 1987, "The kinetic rate of SO2 sorption by CaO", Am. Inst. Chem. Eng. J., Vol. 33, No. 2, pp. 211-217.

Snow, M. J. H., Longwell, J. P. and Sarofim, A. F., 1988, “Direct sulfation of calcium carbonate”, Ind. Eng. Chem. Res., No. 27, pp. 268-273.

Tullin, C., Nyman, G. and Ghardashkhani, S., 1993, “Direct sulfation of $CaCO_3$: the influence of CO_2 partial pressure”, Energy Fuel, No. 7, pp. 512-519.

Van Houte, G. and Delmon, B., 1979, “Kinetics of reaction of $CaCO_3$ with SO_2 and O_2 below 650 °C”, J. Chem. Soc. Faraday Trans. I., No. 75, pp. 1593-1605.

Yrjas, P., Iisa, K. and Hupa, M., 1995, “Comparison of SO_2 capture capacities of limestones and dolomites under pressure”, Fuel, Vol. 74-3, pp. 395-400.

6. Copyright Notice